EPJ Web of Conferences **129**, 00003 (2016) DOI: 10.1051/epjconf/201612900003
QCD@Work 2016

QCD with jets and heavy flavour in pp and PbPb collisions in ATLAS

Robert Keyes[1,⋆] on behalf of the ATLAS collaboration

[1] *McGill University*

Abstract. ATLAS has studied different aspects of QCD in pp and PbPb collisions. A summary of interesting recent results at centre-of-mass energies of 7 TeV, 8 TeV and 13 TeV (pp), and 2.76 TeV (PbPb) per nucleon pair is presented. Using pp collisions, measurements of Z, W, photon, quarkonia and open charm production differential cross sections in a variety of variables are presented. Jet and heavy flavour muon measurements in PbPb collisions, aimed to test the properties of the Quark Gluon Plasma, with the view of better understanding of jet quenching, are also presented.

1 Introduction

The Large Hadron Collider (LHC) is the energy frontier of high energy particle physics, providing the highest energy and highest luminosity environment for proton-proton (pp) and heavy ion (HI) collisions to date. ATLAS is a multipurpose particle detector with a broad physics program that makes use of precision tracking, calorimetry and muon detectors [1]. Signals arising from collisions of coloured constituents of the matter are dominated by Quantum Chromodynamic (QCD) processes. Measuring broad aspects of QCD production provides constraints on QCD theoretical predictions as well as requisites for the empirical description of the proton and its constituents. Finally, having an accurate description of the QCD background of non-QCD measurements, such as Higgs measurements or searches beyond the Standard Model, is critical to their success.

2 Standard Model Boson measurements

2.1 Inclusive W and Z production at 13 TeV

W and Z boson production cross sections are measured at 13 TeV, providing an important benchmark of QCD and electroweak processes that are sensitive to the choice of PDF [2]. The measurements consider leptonic decays in the electron and muon channels: single-lepton with missing transverse energy for W boson candidate events and dilepton that fall within the Z mass window for Z boson candidate events. The primary backgrounds for the W boson measurements are multijets, which are estimated using a data driven approach. The primary backgrounds for the Z boson measurements are diboson signatures (WW), Z to di-tau and top quark decays, all of which are derived from simulations. The

⋆e-mail: rkeyes@cern.ch

measurements display a good agreement with predictions from NNLO QCD and NLO+EW corrections. The electron and muon channels measured separately in each case are found to be consistent. Figure 1 (left), displaying the ratio of predicted to measured cross sections shows tension between different PDFs. In Figure 1 (right), the W^+ to W^- cross section ratio enhances this tension due to cancellations of correlated measurement uncertainties.

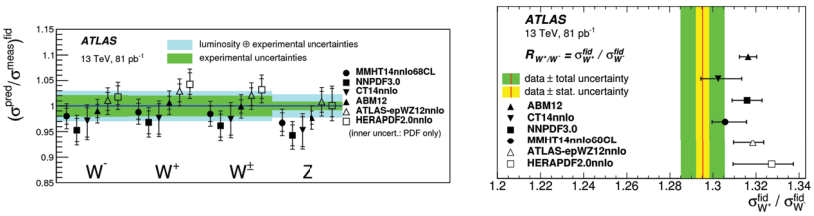

Figure 1. Comparison of the measured and predicted W and Z cross sections (left) and the W^+/W^- ratio of the measured cross-section (right) using various PDF descriptions [2].

2.2 Inclusive Z p_T at 8 TeV

The measurement of the inclusive Z boson p_T spectrum at 8 TeV provides a comprehensive test of QCD predictions spanning the non-perturbative regime at low p_T to the perturbative regime at high p_T [3]. W and Z bosons constitute a significant background in many analyses and previous simulations of these backgrounds have required data-driven corrections [4, 5]. The measurement is conducted by selecting dilepton final states, a clean signature that benefits from a precise p_T determination and low background. Measurements were compared to the predictions from Pythia and Sherpa, as shown in Figure 2 (left), both displaying a poor agreement in the high p_T tail. Comparisons to a higher order pQCD computation DYNNLO yielded a better description of the shape but with a constant offset, as seen in Figure 2 (right).

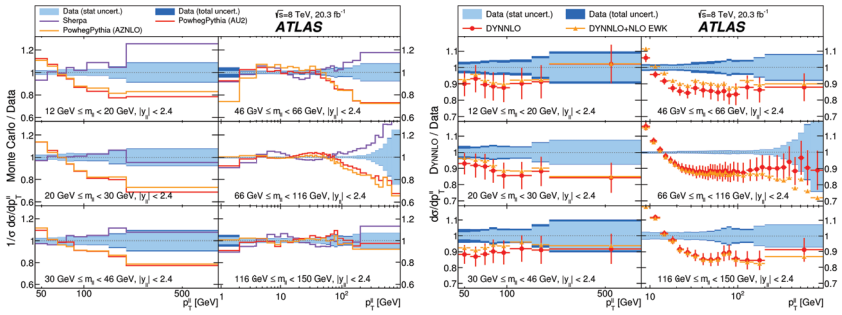

Figure 2. Comparison of the measured cross sections using various generator level descriptions (left) and DYNNLO with and without electroweak corrections (right) [3].

2.3 Inclusive photon E_T at 8 TeV

Prompt photons originating from hard scattering are a clean probe of the parton level dynamics and of the gluon PDF. Arising predominantly through Compton process like $qg \rightarrow q\gamma$ scattering, prompt photon signatures are targeted experimentally by requiring that the photon is isolated, i.e. well separated from other calorimetric signatures. Events simulated using Pythia and CTEQ6L1 PDF are used to correct for detector effects and signal leakage in order to extract the central value of the measurements [6]. A significant improvement in experimental uncertainties, compared to previous results, is obtained thanks to improved photon calibrations [7]. The result is compared to theory predictions at NLO from JetPhox using various PDF sets, and at NLO+NNNLL (which is comparable to NNLO) from PeTeR, as seen in Figure 3. Comparisons yield a good shape agreement and a better normalization with PeTeR. This measurement provides an important constraint on the global fit of the gluon PDF.

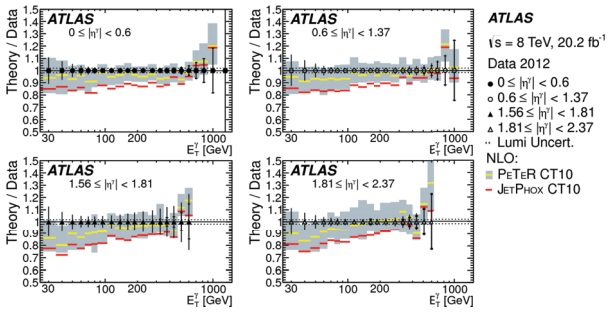

Figure 3. The measured photon E_T differential cross section compared to JetPhox and PeTeR [6].

3 Heavy flavour production measurements

3.1 J/ψ and $\psi(2S)$ at 7 and 8 TeV

Heavy flavour QCD bound states (quarkonia) probe the boundary of perturbative and non-perturbative QCD. Charmonium production can arise through "prompt" short lived sources or through "non-prompt" long lived sources such as the decay of a beauty hadron. The $\psi(2S)$ state is of interest because it is the only vector charmonium state that has mostly direct production. The measurements are performed by selecting di-muon decay events, a final state that exhibits efficient triggering and clean reconstruction [8]. The pseudo-proper time τ observable measures the displacement of the hadron before its di-muon decay, as seen in Figure 4 (left). A two dimensional maximum likelihood fit is performed over the invariant mass and τ, the former discriminating signal from background by isolating the bound state resonance, the latter separating the prompt from the non-prompt components. The results of these cross section measurements agree well with results from other LHC experiment measurements. The comparison of the data to NLO NRQCD predictions for prompt production agree well as seen in Figure 4 (middle), the comparison to FONLL predictions for non-prompt production shows that the predictions slightly overestimate the data at high p_T, as seen in Figure 4 (right).

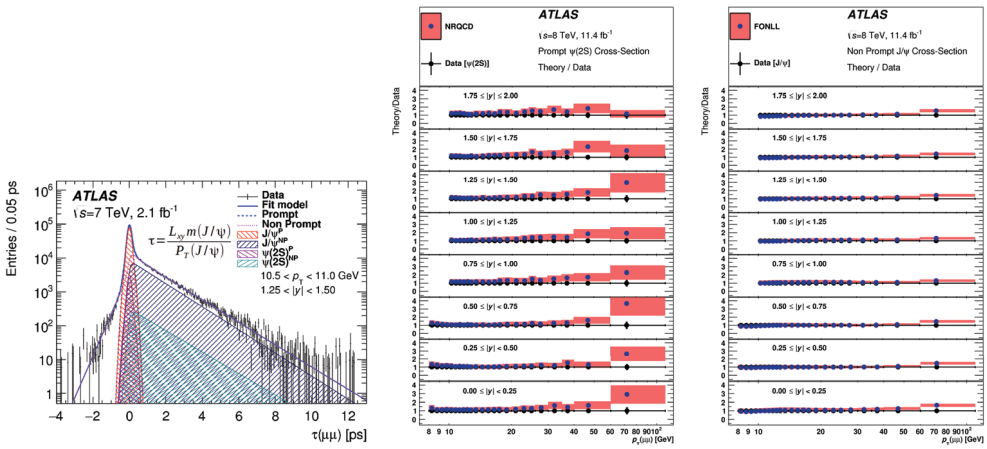

Figure 4. The proper time distribution (left) and comparisons of the measured $\psi(2S)$ (middle) and J/ψ (right) cross section ratios to NRQCD and FONLL predictions [8].

3.2 Prompt and non-prompt J/ψ at 13 TeV

During the long shut down between Run 1 and Run 2 ATLAS installed additional layers of silicon pixel tracking by virtue of shrinking the beam pipe. This new "Inner B Layer" (IBL) provides enhanced vertexing and heavy flavour tagging capabilities in anticipation of more challenging pile-up conditions for Run 2. The ratio of prompt to non-prompt J/ψ production was measured at 13 TeV using a small preliminary dataset [9] and found to be consistent with the Run 1 results in all pseudo-rapidity regions, providing a promising first look of ATLAS heavy flavour performance in Run 2.

3.3 Open charm production at 7 TeV

D mesons arising in the fragmentation of c and b quarks provide a test of pQCD heavy flavour production, of heavy flavour content of the proton, and serve as an important constraint for heavy flavour backgrounds for Higgs measurements. At LHC the charm cross section is large cross and a clean signatures is provided by the precise tracking and vertexing capability of ATLAS [10]. Comparing the results to various predictions, we see that they typically underestimate the data, with FONLL and POWHEG showing the best shape agreement, as shown in Figure 5. The total measured cross section is consistent with those reported by ALICE [11]. The strangeness suppression factor and the charged non-strange vector D-meson fraction are consistent with previous results from ALICE [12].

4 Heavy ion measurements

Heavy Ion (HI) collisions create a hot dense medium of strong nuclear matter with deconfined color charges referred to as the Quark Gluon Plamsa (QGP). This new testing ground for QCD bears an important correspondence to the state and evolution of the early universe. Jet quenching, a recently discovered QGP phenomena, refers to jets interacting with the QGP and becoming more diffuse. Measurements are compared to analogous measurements derived from pp collisions in place of HI simulations. HI collisions are parametrized in terms of the Centrality observable. Centrality is measured in ATLAS using the total energy collected in the forward calorimeters: the more central or

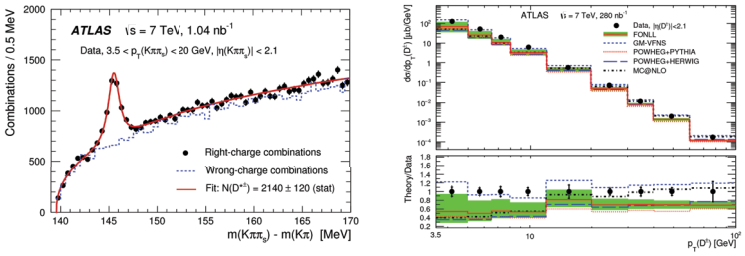

Figure 5. Reconstructed mass peak for the $D^{*\pm}$ meson (left) and the differential cross section in p_T for the $D^{\pm}$ meson (right) [10].

head-on the collision, the more interacting nucleons there are, and in turn, the more outgoing particles and energy deposited [13].

4.1 Dijet p_T correlations in PbPb at 2.76 TeV

Dijets provide a convenient probe of the QGP since in pp collisions they are typically well balanced. The dijet asymmetry, $x_J = \frac{p_T^2}{p_T^1}$, was measured to quantify the effect of jet quenching as a function of jet p_T and centrality [14]. The x_J distribution was found to strongly deviate from the nominal distribution observed in pp collisions with decreasing jet p_T and decreasing collision centrality, as shown in Figure 6 (left). The low p_T and high centrality region show the strongest asymmetry with a peak at $x_J = 0.5$.

4.2 Internal jet structure in PbPb at 2.76 TeV

The internal structure of jets in PbPb collisions is measured to provide constraints on jet quenching models and in-medium modifications for parton shower models [15]. Charged particles with p_T down to 1 GeV falling inside a jet are measured, correcting for tracking inefficiencies. The resulting jet fragmentation functions are reported as a function of longitudinal and transverse charged particle p_T, with respect to the jet axis, in different regions of centrality, jet η and jet p_T. In comparison to pp collision measurements, as shown in Figure 6 (right), an enhancement is observed at low and high charged particle p_T and a suppression in the $4 < p_T < 25$ GeV range. The enhancement at high p_T diminishes with increasing jet p_T and with increasing jet η, and, as would be expected, all the effects diminish with decreasing centrality.

4.3 Heavy flavour muons in PbPb

Heavy flavour signals are produced perturbatively in the hard scatter (as their masses are much greater than the temperature of the medium) and subsequently interact with the medium [16]. Heavy flavour muons are identified using an energy loss variable that takes the difference between the p_T measured by the inner detector and by the muon system. The yields show a centrality dependent suppression that is slightly more significant than that measured by the inclusive jet HI result [17]. Following its creation the QGP expands and cools. By measuring the distribution of the heavy flavour muons in azimuthal angle ϕ, the azimuthal anisotropy, relevant to elliptical flow, is extracted by fitting a 2^{nd} order Fourier coefficient, v_2. v_2 is measured to be up to 8% at low p_T and the overall variation is consistent with previous measurements [18]. Overall the findings are consistent with, and much more precise than, measurements performed by ALICE in the forward region ($2.5 < y < 4.0$) [19].

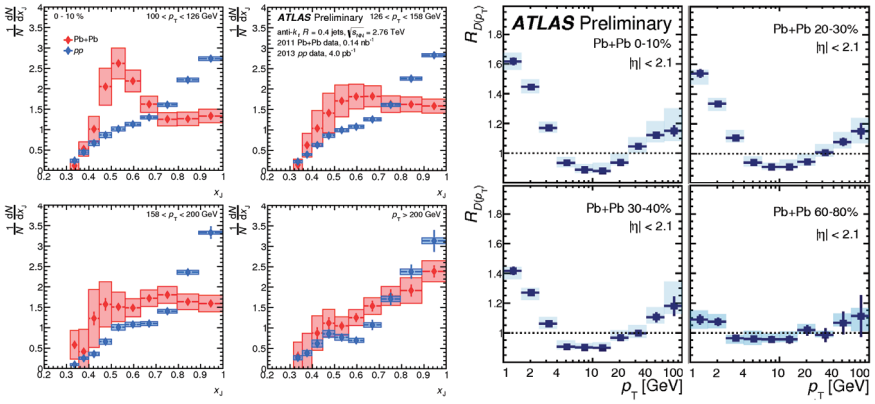

Figure 6. Comparison of the measured dijet asymmetry $x_J = \frac{p_T^2}{p_T^1}$ in PbPb to pp (left) [14], and the ratio of the jet fragmentation functions measured in PbPb to pp (right) [15], in different centrality regions. Statistical uncertainties are displayed using error bars while systematic uncertainties use shaded boxes.

5 Conclusions

The ATLAS experiment has a comprehensive program of QCD studies in the contexts of Standard Model, Heavy Flavour and HI. These results emphasise that ATLAS is performing well, providing new and extended measurements, which are cross checks with previous results. Simulations have also progressed considerably but improvements are still needed, motivating these and future studies.

References

[1] ATLAS Collaboration, JINST **3**, S08003 (2008).
[2] ATLAS Collaboration, Phys. Lett. B **759**, 601 (2016).
[3] ATLAS Collaboration, Eur. Phys. J. C **76**, 291 (2016).
[4] ATLAS Collaboration, J. High Energy Phys. **1**, 69 (2015).
[5] ATLAS Collaboration, ATLAS-CONF-2014-038, https://cds.cern.ch/record/1735215 (2014).
[6] ATLAS Collaboration, J. High Energy Phys. **8**, 5 (2016).
[7] ATLAS Collaboration, Phys. Rev. D **89**, (2014).
[8] ATLAS Collaboration, Eur. Phys. J. C **76**, 283 (2016).
[9] ATLAS Collaboration, ATLAS-CONF-2015-030, https://cds.cern.ch/record/2037967 (2015).
[10] ATLAS Collaboration, Nucl. Phys. B **907**, 717 (2016).
[11] ALICE Collaboration, J. High Energy Phys. **7**, 191 (2012).
[12] ALICE Collaboration, J. Phys. Lett. B **718**, 279 (2012).
[13] ATLAS Collaboration, Phys. Rev. Lett. **105**, 252303 (2010).
[14] ATLAS Collaboration, ATLAS-CONF-2015-052, https://cds.cern.ch/record/2055673 (2015).
[15] ATLAS Collaboration, ATLAS-CONF-2015-055, https://cds.cern.ch/record/2055676 (2015).
[16] ATLAS Collaboration, ATLAS-CONF-2015-053, https://cds.cern.ch/record/2055674 (2015).
[17] ATLAS Collaboration, Phys. Rev. Lett. **114**, (2015).
[18] ATLAS COllaboration, Phys. Rev. C **86**, (2012).
[19] ALICE Collaboration, Phys. Rev. Lett. **109**, (2012).